Diagnostic and screening potential of plasma exosome miR-99b-5p and its combination with other miRNAs for colorectal cancer

CHANG ZHANG[1,2*], LIMEI ZHANG[3*], QIYUAN HUANG[4], SIYUAN JIANG[3], TAO PENG[5], SHU WANG[6] and XUEHU XU[3]

[1]Center of Clinical Aerospace Medicine, School of Aerospace Medicine, Key Laboratory of Aerospace Medicine of Ministry of Education; [2]Department of Aviation Medicine, The First Affiliated Hospital, Air Force Medical University, Xi'an, Shanxi 710032; [3]Department of Gastrointestinal Surgery, The Third Affiliated Hospital of Guangzhou Medical University, Guangzhou, Guangdong 510150; [4]Nursing School, Guangzhou Medical University, Guangzhou, Guangdong 510030; [5]Sino-French Hoffmann Institute, Guangzhou Hoffman Institute of Immunology, School of Basic Medical Sciences, Guangzhou Medical University, Guangzhou, Guangdong 511436, P.R. China; [6]Department of Biological Sciences, National University of Singapore, Singapore 117543, Republic of Singapore

Received July 21, 2023; Accepted February 15, 2024

DOI: 10.3892/ol.2024.14594

Abstract. Extracellular vesicles (EVs) secreted by tumor cells have been documented to hold viable biomarker potential. Therefore, the present study evaluated the potential clinical value of EV-microRNAs (miRNAs or miRs) in the plasma exosomes of patients with colorectal cancer (CRC) for the early diagnosis and screening of CRC. In total, 95 plasma samples were collected at The Third Affiliated Hospital of Guangzhou Medical University (Guangzhou, China) between 2017 and 2019. Specifically, 68 samples were from patients with CRC and 27 were from healthy control (HC) donors. High-throughput sequencing was used to detect the expression of miRNAs in the isolated plasma EVs, which was subsequently verified by reverse transcription-quantitative PCR. Receiver operating characteristic (ROC) curves were used to analyze the diagnostic potential of single and combined miRNAs for CRC. Bioinformatics analysis was employed to predict the target genes of candidate miRNAs. Compared with those in the HC group, the CRC group expressed higher levels of miR-99b-5p and miR-409-3p, especially during the early stages of CRC. Clinicopathological analysis confirmed the higher expression levels of miR-99b-5p during the early stages, as well as higher expression levels in the colon compared with those in the rectum. ROC curve analysis revealed that the area under the curve (AUC) of miR-99b-5p for the diagnosis of early CRC was 73.5% (P=0.007). The early diagnostic capability of miR-99b-5p combined with miR-409-3p for CRC was evaluated, and the AUC was found to be 74.1% (P=0.006). In addition, the AUC of the combination of miR-99b-5p, miR-409-3p and carcinoembryonic antigen was 81.2% (P<0.001), indicating that this three-parameter combination displayed higher diagnostic power compared with any single miRNA for early CRC screening. The results from the present study suggest that the expression of miR-99b-5p in plasma exosomes is significantly upregulated in CRC, which holds potential for the early diagnosis of this cancer type. Such potential can be enhanced further by combining it with other miRNAs. Therefore, the present study provides a comprehensive but preliminary insight for the viability of miR-99b-5p (alone or combined with other miRNAs) for CRC diagnosis, which requires further exploration in the future.

Correspondence to: Professor Xuehu Xu, Department of Gastrointestinal Surgery, The Third Affiliated Hospital of Guangzhou Medical University, 63 Duobao Road, Liwan, Guangzhou, Guangdong 510150, P.R. China
E-mail: xxh@gzhmu.edu.cn

*Contributed equally

Key words: colorectal cancer, plasma exosomes, early diagnosis, microRNA-99b-5p, microRNA-409-3p

Introduction

Colorectal cancer (CRC) is a malignancy of the colon or rectum, with high incidence and mortality rates (1). CRC is relatively common in China, with an annual incidence of 398,000 cases and an annual mortality rate of 188,000 cases, which causes notable national economic burden (2). Since the symptoms of CRC remain subclinical during the early stages of the disease, early diagnosis is difficult, which is why at the time of diagnosis, the majority of patients are already in the advanced stages of the disease. However, compared with advanced CRC (III-IV), it was previously reported that the 5-year survival rate of CRC could be significantly improved (up to 90%) by timely treatment in the early stages (3-5). Therefore, early diagnosis and treatment are essential for the prevention of CRC progression.

Current diagnostic strategies that are clinically used for detecting CRC and precancerous lesions include colonoscopy, stool testing, carcinoembryonic antigen (CEA), colonography, computed tomography and double-contrast barium

enemas (6). In particular, colonoscopy is considered to be the gold standard for CRC diagnosis, enabling its early discovery. However, it is an invasive procedure that can be uncomfortable for patients, and has various limitations, such as the difficulty of collecting samples, small pathological sample size and complicated multiple sampling (7). Therefore, this method cannot be popularized for CRC screening. By contrast, the use of serum tumor markers such as CEA may be beneficial for the prognostic evaluation of this disease; however, CEA cannot be used for early diagnosis of CRC, since there may be no obvious changes in the levels of serum markers during the early stages of this malignancy (8). Consequently, there is currently an unmet clinical demand for novel diagnostic markers for early-stage CRC that are highly specific and sensitive but less traumatic.

Accumulating evidence has suggested that the expression levels of various microRNAs (miRNAs or miRs) are associated with tumor initiation, progression, and prognosis. In particular, circulating miRNAs have been proposed to serve as potential biomarkers in different types of cancer (9). Changes in the levels of circulating miR-21, miR-92 and miR-141 have been documented to correlate with those of other well-established CRC markers such as epidermal growth factor receptor (EGFR), cytokeratin (CK)20, CK19 and CEA for providing sensitive early diagnosis (10). At the same time, the miRNA expression profile typically varies according to the molecular phenotype of the tumor in question, which may affect prognosis.

miR-99b-5p and miR-196b-5p have been reported to be closely associated with the survival rates of patients with microsatellite instability in colon and rectal cancer (11). Extracellular vesicles (EVs) are vesicles with intact membrane structures that are naturally secreted from cells, with diameters ranging from 30 to 1,000 nm. Although almost all cell types can secrete exosomes, tumor cells tend to produce more exosomes compared with their non-cancerous counterparts. In addition, exosomes from tumor cells appear to be more stable. Therefore, it would be beneficial to identify novel biomarkers or even novel therapeutic targets that are associated with tumor cell exosomes (12,13). Since tumor cell exosomes can carry tumor information, the expression profiles of plasma exosome miRNAs (EV-miRNA) of patients with cancer are likely to be tumor-specific, which can in turn be exploited to reflect disease characteristics by comparing them with the profile of circulating total miRNAs (14).

In the present study, the EV-miRNA profile of patients with CRC was characterized using RNA sequencing before evaluating its diagnostic potential. Subsequently, specific miRNAs of interest were tested either alone or in different combinations for their viability as diagnostic markers of early-stage CRC.

Materials and methods

Patients and clinical samples. The present study involved 68 patients with CRC (clinicopathological stages I-IV) and 27 healthy control (HC) individuals (15). The patients were admitted to the Department of Gastrointestinal Surgery, The Third Affiliated Hospital of Guangzhou Medical University (Guangzhou, China) between March 2017 and June 2019. The present study was prospective and was approved by Ethics Committee of the Third Affiliated Hospital of Guangzhou Medical University (Guangzhou, China; approval no. 2017.117), including the use of all datasets. Written informed consent was obtained from all participants.

Among the patients with CRC, 41 were males and 27 were females, with an age range of 38-77 years. The 27 HC individuals were selected from healthy subjects who visited the Third Affiliated Hospital of Guangzhou Medical University during the same period of time, of whom 12 were males and 15 were females, with an age range of 58-68 years. A total of 16 patients were enrolled in the screening period, 12 patients with CRC and 4 HC individuals; 79 patients were enrolled in the validation period, 56 patients with CRC and 27 HC individuals. Differences in sex, age and other general data between the two groups were not statistically significant (Table I).

The inclusion criteria were as follows: i) Age >18 years with no mental impairments; ii) histopathologically or cytologically confirmed CRC; and, for HC individuals, iii) no CRC or adenoma found by electronic colonoscopy. The exclusion criteria were as follows: Patients who i) exhibited ≥2 types of primary solid tumor; ii) had received chemoradiotherapy, surgery or systemic steroid therapy within the last 3 months; iv) were diagnosed with other serious diseases, or suffered from systemic active infection requiring treatment, immunodeficiency, autoimmune diseases and/or severe allergic diseases; and v) were pregnant or lactating women. All patients with CRC were diagnosed by histopathological analysis of surgically resected tissues or by electronic colonoscopy combined with histopathological biopsy. Pathological diagnosis and confirmation in tissue specimens were performed by ≥2 pathologists. Briefly, 5 ml fasting peripheral blood (collected after fasting for ≥8 h) was collected from patients with CRC and healthy subjects, and blood samples were processed within 2 h of collection. Immediately after blood collection, the samples were inverted and mixed well 5-8 times, before being placed at 25˚C, followed by centrifugation at 3,500 x g for 10 min at 25˚C within 2 h. The supernatants, i.e. plasma, were then carefully collected in cryovials and frozen at -80˚C until further use.

Plasma exosome isolation. Plasma exosomes were extracted using exoRNeasy Midi Kit (cat. no. 77144; Qiagen GmbH), according to the manufacturer's instructions. The plasma samples frozen at -80˚C were thawed at room temperature and centrifuged at 3,000 x g for 15 min at 4˚C. In total, 1 ml supernatant was collected and decanted into a new Eppendorf tube (Eppendorf SE), to which 400 μl buffer XE was added. The tube was then thoroughly mixed and incubated at 25˚C for 1 min, followed by centrifugation at 3,000 x g for 5 min at 25˚C. Next, the supernatant was discarded and the sample was again subjected to centrifugation at 3,000 x g for 5 min at 25˚C. Finally, the remaining pellet was considered to be the exosome fraction. The obtained samples were then aliquoted and frozen for storage at -80˚C.

Plasma exosome identification. Plasma exosomes were observed under transmission electron microscopy (TEM). Briefly, 5 μl exosome suspension was added to 200 mesh copper grids for 20 min at 25˚C. Excess suspension was removed with filter paper and then fixed with 2% paraformaldehyde

Table I. Plasma sample information.

	Sex, number of subjects		Age, years	
Sample	Male	Female	Mean	Range
HC	12	15	63	58-68
CRC	41	27	62	38-77
Stage 0-II	16	12	59	38-72
Stage III-IV	25	15	64	56-77

Statistical analysis of two-sample data was performed using χ^2 test and independent samples t-test. P-values were all >0.05. Differences in sex and age between the two groups were not statistically significant.

for 20 min at 25˚C. The grids were then washed 10 times with PBS and fixed with 1% glutaraldehyde at 4˚C for 2 h before being washed 10 times with water. The exosomes were negatively stained with 4% uranyl acetate for 10 min at 25˚C, air dried and then visualized using TEM (JEM-1400PLUS; Hitachi, Ltd.) at 80 kV. Plasma EV nanoparticle tracking analysis (NTA) was performed to measure the exosome sizes in all samples. Protein concentration was determined using the Pierce™ BCA Protein Assay Kit (Thermo Fisher Scientific, Inc.) at a concentration range of 125-2,000 μg/ml.

Identification of protein expression in plasma exosomes was performed by western blot analysis. Isolated plasma exosomes were resuspended in RIPA buffer [0.05 M Tris-HCl (pH 8), 0.15 M NaCl, 1% Triton X-100, 0.1% sodium deoxycholate and 0.1% sodium dodecyl sulfate] with a protease inhibitor (Roche Diagnostics), and then lysed on ice for 15 min and boiled in 1X SDS sample buffer for 15 min. Protein samples (100 μg) were loaded, separated by SDS-PAGE on 12% gels and transferred to polyvinylidene difluoride membranes, followed by blocking with 5% non-fat milk in TBS-0.05% Tween-20 (TBST) for 1 h at 25˚C. Subsequently, the membranes were incubated overnight with primary antibodies at 4˚C, before being washed with TBST and incubated with secondary antibodies for 1 h at 25˚C. The membranes were then washed again and visualized using enhanced chemiluminescence (ECL) reagent (Pierce ECL Western Blotting Substrate; Thermo Fisher Scientific, Inc.). The antibodies used for western blot analysis are listed in Table II.

Total RNA extraction from plasma exosomes. Total RNA from exosomes was isolated using exoRNeasy Midi Kit (Qiagen GmbH) following the manufacturers' instructions. The resulting total RNA samples were used for reverse transcription-quantitative PCR (RT-qPCR).

High-throughput sequencing. The concentration and RNA integrity of the total RNA from plasma EVs were respectively determined using Qubit (Guangzhou IGE Biotechnology Ltd.) and Agilent 2200 TapeStation (Agilent Technologies, Inc.), respectively, prior to library construction. Small RNA libraries were prepared using the NEBNext Small RNA Library Prep Set for Illumina (New England BioLabs, Inc.) according to the manufacturer's protocol. Briefly, 3' adapters were ligated to the input RNA followed by hybridization of reverse transcription primers and ligation of 5' adapters. RNA was reverse transcribed and amplified by PCR (15 cycles). The PCR amplification products were purified by agarose gel electrophoresis and were then assessed using the Agilent 2200 for quality control. Next-generation sequencing (50 bp, single end) of the small RNA libraries was then performed on an Illumina HiSeq 2500 sequencer (Illumina, Inc.), and the raw data were subjected to a quality assessment to determine their suitability for bioinformatics analysis. Specifically, the quality analysis mainly included sequencing quality and base quality analyses. After Illumina HiSeq 2500 sequencing yielded raw reads, the raw reads were filtered: Adapters at both ends of reads were removed, reads with fragment lengths <17 nt and low-quality reads were removed, and preliminary filtering of the data was completed to obtain filtered clean data. This step was performed using Trimmomatic (Version 0.36; http://www.usadellab.org/cms/?page=trimmomatic). The filtered clean data were then aligned and annotated to known non-coding RNA (ncRNA) databases: miRBase version 22 was used as the miRNA database (16), while Rfam12.1 (17) was the database used for transfer RNA, ribosomal RNA (rRNA), small nuclear RNA and small nucleolar RNA, and piRNABank (18) was the database used for P-element induced wimpy testis in *Drosophila*-interacting RNAs. The annotation results were then statistically compared and graphically presented. Calculations of expression levels were performed on the identified miRNAs. Based on all miRNA expression data, correlation analysis between samples was performed on the sequenced samples. Pearson's correlation coefficient (r) was used to measure the correlation between two variables. The closer the absolute r-value is to 1, the higher the correlation in expression levels between the two samples. A positive r-value was considered to represent positive correlation in the expression patterns between two samples, whilst a negative r-value was considered to represent negative correlation between two samples. Through principal component analysis, the data were analyzed to evaluate the association among the samples, whilst assessing if a specific role was mediated by samples found in different groups. Differential miRNA expression analysis was performed using the 'edgeR' R language package (19).

RT-qPCR. Exosomal RNA was extracted using the miRNeasy advanced kit (Qiagen GmbH) and miRNA levels in plasma EVs were quantified using RT-qPCR. The poly-(A)-tailing method was used for first-strand cDNA synthesis using a miRcute Plus miRNA First-Strand cDNA kit (cat. no. KR211; Tiangen Biotech Co., Ltd.) according to the manufacturer's instruction. RT-qPCR for miRNA quantification was performed using a miRcute Plus miRNA qPCR kit (SYBR Green) (cat. no. FP411; Tiangen Biotech Co., Ltd.) following the manufacturer's protocol. The qPCR thermocycling conditions were as follows: Pre-denaturation at 95˚C for 15 min, followed by five cycles at 94˚C for 20 sec, 65˚C for 30 sec and 72˚C for 34 sec for the enrichment of low-abundance target miRNAs, and 40 cycles at 94˚C for 20 sec and 60˚C for 34 sec for amplification of target miRNAs. Melting curve analysis was performed by heating samples from 65 to 97˚C at a ramp rate of 0.11˚C/sec. The sequences of the primers used in qPCR are

Table II. Antibodies used in western blot analysis.

Antibody name	Cat. no.	Dilution	Supplier
Anti-CD63 antibody	MA5-31276	1:1,000	Thermo Fisher Scientific, Inc.
Anti-CD81 antibody	EXOAB-CD81A-1	1:1,000	System Biosciences, LLC
Anti-TSG101 antibody	ab125011	1:1,000	Abcam
Anti-Alix antibody	PA5-95321	1:1,000	Thermo Fisher Scientific, Inc.
HRP-conjugated goat anti-mouse antibody	RGAM001	1:5,000	Proteintech Group, Inc.
HRP-conjugated goat anti-rabbit IgG H&L	ab6721	1:5,000	Abcam

TSG101, tumor susceptibility gene 101.

Table III. Primer sequences for RT-quantitative PCR.

Primer	Sense	Sequence (5'-3')
hsa-miR-625-3p	Forward	CGCGCGACTATAGAACTTTCCCCCTCA
hsa-miR-409-3p	Forward	GCGAATGTTGCTCGGTGAACCCCT
hsa-miR-143-3p	Forward	CGCGCTGAGATGAAGCACTGTAGCTC
hsa-miR-122-5p	Forward	GCCGCTGGAGTGTGACAATGGTGTTTG
hsa-miR-99b-5p	Forward	CCACCCGTAGAACCGACCTTGCG
hsa-miR-16-5p	Forward	GCGCGTAGCAGCACGTAAATATTGGCG
Reverse primer	Reverse transcription universal primer	GCTGTCAACGATACGCTACGTAAC

RT, reverse transcription; miR, microRNA; hsa, *Homo sapiens*.

shown in Table III. The quantitative cycle (Cq) value was used to perform the relative quantification of miRNA expression as follows: ΔCq=Cq (candidate miRNA)-Cq (reference miRNA). Subsequently, the $2^{-\Delta\Delta Cq}$ method was used to describe the differences in the relative expression levels of miRNA among the different groups (20). The data in the HC group were then normalized to 1, before fold-change (FC) was used to describe the fold-difference in the relative expression of miRNAs in the CRC and HC groups as follows: $FC=2^{-\Delta\Delta Cq}=2^{-\Delta Cq}$ (reference group)/$2^{-\Delta Cq}$ (analyzed group). miR-16-5p was used as an internal reference miRNA (21). The expression stability of miR-16-5p in plasma EV-RNA samples was confirmed by analyzing the relative expression of miR-16-5p in each sample. Namely, miR-16-5p was consistently expressed in each sample.

Statistical analysis. GraphPad Prism7 software (GraphPad; Dotmatics) and SPSS 25.0 (IBM Corp) were used for statistical analysis and mapping of relative miRNA expression. Preliminary bar graphs were prepared using Excel 2019 (Microsoft Corporation). Measurement data are expressed as the mean ± SD. Independent samples Student's t-test was used for the statistical analysis of two-group unpaired data with equal variance. Corrected Welch's t-test would be used if the variance was found to be unequal. Logistic regression analysis was used for risk factor analysis, where odds ratio (OR) was obtained. OR >1 would be considered to indicate that a factor is a risk factor for the tested outcome events, whereas OR <1 would be considered to indicate that a factor is a protective factor against the tested outcome events. Receiver operating characteristic (ROC) curves were used to assess the diagnostic potential of miRNAs for CRC. Youden's index maximum value was used to determine the sensitivity and specificity corresponding to the cut-off value of the CRC curve as follows: Youden index=(Sensitivity + specificity)-1. A miRNA combination model was developed using multivariate logistic regression analysis. The diagnostic potential of miRNA combinations for CRC was assessed in combination with the ROC curves. $P<0.05$ was considered to indicate a statistically significant difference.

Results

Characterization of exosomes isolated from plasma of patients with CRC. Plasma exosomes were extracted from patients with CRC using the aforementioned exoRNeasy Midi Kit and were observed using TEM. The particles were evenly distributed and displayed several micromembrane-coated vesicular structures, with a single distribution and a double-layered membrane structure, suggesting that exosomes were successfully obtained (Fig. 1A and B).

The particle size distribution and concentration of EV sample particles were determined using NTA. The results revealed that 97.6% of EV particles were distributed around 163.9 nm, with an average EV particle size of 168 nm (Fig. 1C). EV marker proteins were next assessed using western blotting, revealing that common marker proteins of EVs, namely CD63,

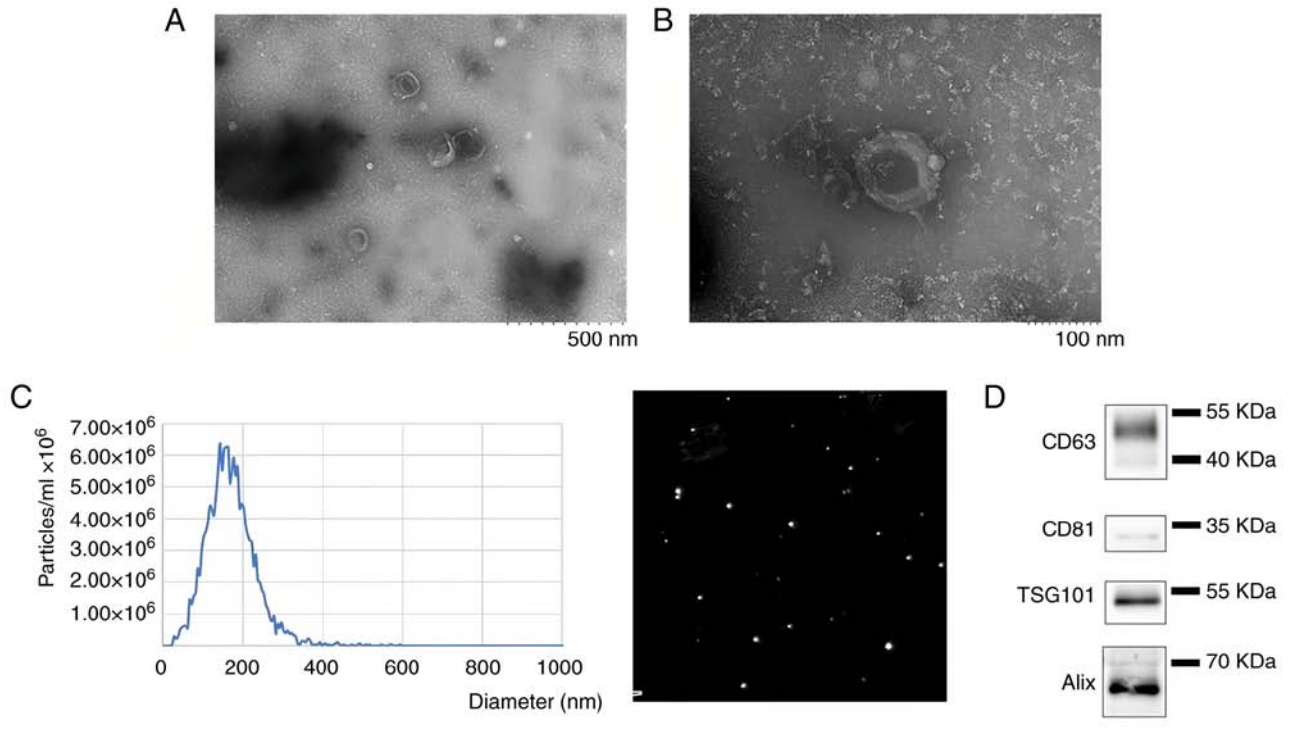

Figure 1. Identification of plasma EVs. (A and B) Observation of EVs by transmission electron microscopy. (A) Scale bar, 500 nm. (B) Scale bar, 100 nm. (C) Nanoparticle tracking analysis. Left, sample EV particle size distribution map; right, display of particles in the nanoparticle tracking analysis detection window. Maximum area, 1,000 nm; minimum area, 5 nm; minimum brightness, 20 nm. (D) Qualitative detection of CD63, TSG101, Alix and CD81 proteins by western blotting. EV, extracellular vesicle; TSG101, tumor susceptibility gene 101.

CD81, TSG101 and Alix (22), were present on EV membranes (Fig. 1D). In addition, tumor susceptibility gene 101 and Alix proteins, which are commonly found EV markers (22), were found to be expressed (Fig. 1D). These results suggested that plasma exosomes were successfully extracted.

High-throughput sequencing for screening of plasma exosomal miRNAs. In total, 16 plasma samples, collected from 12 patients with CRC and 4 HC individuals, were subjected to total RNA extraction from the isolated EVs, followed by high-throughput sRNA sequencing. The 16 samples were grouped according to the clinicopathological characteristics of the participants (Table IV). As shown in Table V, all samples had >11 million raw reads, >10 million filtered clean reads and Q30 of raw reads >85% for all samples, suggesting that the raw and filtered data obtained by sequencing were of sufficient quality for subsequent bioinformatics analysis (16). The clean reads obtained by sequencing were analyzed using miRBase. Alignment with all human miRNA mature sequences in the miRBase version 22 database (12) provided information on the structure, length and expression of the miRNAs. In total, 458-698 mature miRNAs were aligned in each of the 16 samples, as shown in Table VI.

Next, differential miRNA expression analysis was performed using the 'edgeR' software package using the following two criteria: $|\log_2(FC)|>1$ and $P<0.05$. By using this method, miRNAs that were differentially expressed among the different groups were found. Grouping was performed based on the clinicopathological parameters of the 16 sequenced samples, and multiple pairwise comparisons were performed to obtain miRNAs that were differentially expressed among different groups and had a mean read per million (RPM) value of >100 in 16 samples (Table VII). The mean RPM expression values of the aberrantly expressed miRNAs in the 16 samples was $\log_2$-transformed, before the relative mean expression value of the miRNAs of interest in the 16 plasma EV-RNA samples was plotted as a bar chart (Fig. 2). Since the plasma EV-miRNA abundance is of particular importance for the quantitative detection of miRNAs, we combined the two factors: miRNA expression difference results between groups and expression abundance, to select five miRNAs with significant differential expression between groups from the differential analysis results, and all five miRNAs were expressed in high abundance in samples for subsequent clinical plasma sample validation. Five miRNAs, namely miR-122-5p, miR-409-3p, miR-99b-5p, miR-625-3p and miR-143-3p, were selected for validation, since they exhibited significant differential expression and high expression levels in the analyzed samples (Fig. 2).

Differential analysis of miRNA expression and validation by RT-qPCR. The expression levels of the aforementioned five candidate miRNAs (miR-122-5p, miR-409-3p, miR-99b-5p, miR-625-3p and miR-143-5p) in the 79 plasma EV samples from patients with CRC and healthy individuals were determined using RT-qPCR. There were 56 samples in the CRC group and 23 samples in the HC group. The FC in miRNA expression levels in the CRC group compared with the HC group was then calculated. As shown in Fig. 3A and B, miR-99b-5p and miR-409-3p were respectively found to

Table IV. Grouping of 16 sequencing samples.

Group name	Clinicopathological characteristic	Samples, n	Sample name
g1g2	CRC	12	A1, A5, A7, A8, A9, A10, B4, B5, B6, B7, B8, B9
g1	Early CRC	6	A1, A5, A7, A8, A9, A10
g2	Advanced CRC	6	B4, B5, B6, B7, B8, B9
g3	0-Phase I	3	A1, A5, A7
g4	Phase II	3	A8, A9, A10
g5	Liver metastases	4	B4, B5, B6, B8
Control	Healthy controls	4	N5, N6, N7, N8
B79	Abdominal metastasis	2	B7, B9

CRC, colorectal cancer; g, group no.; A, stage 0-II; B, stage III-IV; N, healthy controls.

Table V. Raw data quality.

Samples	Raw reads	Raw bases, nt	Read length, nt	GC, %	Q20, %	Q30, %	Clean reads	Clean rate, %
A1	11,932,170	596,608,500	50	53.35	96.77	93.46	11,022,867	92.38
A10	12,607,148	630,357,400	50	52.64	96.81	93.32	11,452,454	90.84
A5	12,969,621	648,481,050	50	52.94	96.23	92.03	10,611,851	81.82
A7	11,626,050	581,302,500	50	53.65	97.1	94.04	11,001,737	94.63
A8	12,084,325	604,216,250	50	53.29	96.83	93.49	11,024,278	91.23
A9	11,952,800	597,640,000	50	53.52	96.88	93.61	11,004,699	92.07
B4	11,969,375	598,468,750	50	53.47	96.85	93.59	11,002,397	91.92
B5	13,054,681	652,734,050	50	52.31	96.63	92.76	10,105,612	77.41
B6	12,029,175	601,458,750	50	52.92	96.68	93.21	11,010,671	91.53
B7	16,275,700	813,785,000	50	53.01	95.9	92.26	11,172,706	68.65
B8	13,860,500	693,025,000	50	53.26	94.46	88.55	10,825,737	78.10
B9	13,771,725	688,586,250	50	53.37	94.39	88.53	10,760,592	78.14
N5	12,069,725	603,486,250	50	53.33	96.71	93.3	11,003,428	91.17
N6	13,353,690	667,684,500	50	53.07	96.71	93.26	11,917,798	89.25
N7	13,569,100	678,455,000	50	53.34	94.68	89.08	10,869,726	80.11
N8	13,554,675	677,733,750	50	53.37	95.02	89.83	10,913,743	80.52

GC%, the proportion of cytosine and guanine in the complete genome of organisms, as a percentage of all bases. Q20 corresponds to an error rate of 1%. Q30 corresponds to an error rate of 0.1%. Q, base quality value. A, stage 0-II; B, stage III-IV; N, healthy controls.

be significantly increased in the CRC group compared with the HC group (P<0.05). Differences in expression were also observed between the CRC and HC groups for miR-122-5p, miR-143-3p and miR-625-3p (Fig. 3C-E), but without statistical significance. These results suggest that miR-99b-5p may be a useful marker for diagnosis of CRC.

Association of miRNA expression levels with clinicopathological features. To further evaluate the significance of miRNAs expression profiles, the miRNA expression levels in CRC samples of patients with different pathological features were compared. As shown in Table VIII, the expression levels of miR-99b-5p were found to be different among different clinical stages and lesion sites of CRC. As shown in Fig. 4, among the various clinical stages of CRC, the expression levels of miR-99b-5p were significantly higher during early CRC compared with advanced CRC (P=0.03). And the expression levels of miR-409-3p were higher during early CRC compared with in the HC group (P<0.05; Fig. 5). Furthermore, exosomal miR-99b-5p expression levels were significantly higher in patients with CRC originating from the colon compared with those in CRC originating from the rectum (P=0.028; Fig. 6A), which suggests that exosomal miR-99b-5p may be an indicator of early CRC pathogenesis or progression. CRC located in the proximal colon (right) and distal colon (left) were previously found to exhibit different molecular characteristics and histology, suggesting that the pathogenesis of CRC depends on tumor location (23). In the present study, exosomal miR-625-3p expression levels were significantly higher in right-sided CRC compared left-sided CRC (P=0.007; Fig. 6B), suggesting that exosomal miR-625-3p may also serve as a biomarker for CRC pathogenesis. Using logistic regression analysis for assessing

Table VI. Expression of miRNAs in each sample.

Sample name	miRNA, n
A1	639
A5	675
A7	465
A8	458
A9	503
A10	476
B4	539
B5	600
B6	605
N5	481
N6	639
N7	635
N8	606
B7	698
B8	596
B9	597

miRNA, microRNA. A, stage 0-II; B, stage III-IV; N, healthy controls.

the potential risk factors of early CRC, it was found that high miR-99b-5p expression may be a risk factor of early CRC, with an odds ratio of 2.725 and a 95% confidence interval (CI) of 1.236-6.008 (P=0.013) (data not shown).

ROC curve analysis of the diagnostic potential of individual miRNAs for CRC. ROC curves were constructed for the differentially expressed miRNAs in plasma EVs to assess their diagnostic potential for CRC. Specifically, 95% CI and area under the curve (AUC) values were obtained. The maximum Youden index value was used to determine the sensitivity and specificity corresponding to the cut-off value of the respective ROC curves. ROC curve analysis was first performed individually for the differentially expressed miRNAs in the CRC group. As shown in Fig. 7A, miR-99b-5p yielded an AUC of 0.660 (95% CI, 0.527-0.793; sensitivity, 55.4%; specificity, 78.3%; P=0.026). This result suggested that miR-99b-5p had potential for the diagnosis of CRC in HC individuals, and its diagnostic specificity could reach 78.3%. However, its diagnostic sensitivity was only 55.4%.

On the other hand, miR-409-3p yielded an AUC of 0.604 (95% CI, 0.471-0.737; sensitivity, 58.9%; specificity, 80.2%; P=0.148), suggesting that this miRNA had limited diagnostic ability for CRC (Fig. 7B). ROC curve analysis of the differentially expressed miR-99b-5p in the early CRC group revealed that it had a higher differential diagnostic potential for early CRC, where its AUC reached 0.735, and its sensitivity and specificity both reached >70% (Fig. 7C). Specifically, miR-99b-5p yielded an AUC of 0.735 (95% CI, 0.587-0.884; sensitivity, 72.7%; specificity, 78.3%; P=0.007; Fig. 7C). ROC analysis of miR-409-3p for early CRC revealed an AUC of 0.611 (95% CI, 0.443-0.778; sensitivity, 63.6%; specificity, 60.9%; P=0.204; Fig. 7D). The performance of CEA, which is used clinically for the diagnosis of early CRC, yielded an AUC of 0.820 (95% CI, 0.695-0.945; sensitivity, 72.7%; specificity, 87%; P<0.001; Fig. 7E).

ROC curve analysis of the diagnostic potential of miRNA combinations for CRC. To explore whether multiple miRNAs in combination could improve the diagnostic potential for CRC, a regression analysis model of various miRNAs was developed. The diagnostic potential of these miRNAs was then analyzed using ROC curves, which revealed that the diagnostic performance for CRC of multiple miRNAs in combination was superior compared with that of individual miRNAs. In particular, the combination of miR-99b-5p and miR-409-3p (Fig. 8A) was evaluated for the diagnosis of early CRC, yielding an AUC of 0.673 (95% CI, 0.542-0.804; sensitivity, 66.1%; specificity, 73.9%; P=0.016). In addition, the combination of CEA and miR-99b-5p for the diagnosis of early CRC was found to exert superior diagnostic efficacy, yielding an AUC of 0.863, (95% CI., 0.774-0.952; sensitivity, 83.6%; specificity, 82.6%; P<0.001; Fig. 8B). When the miR-99b-5p and miR-409-3p combination was applied for the diagnosis of early CRC, an AUC of 0.741 was found (95% CI, 0.592-0.891; sensitivity, 77.3%; specificity, 78.3%; P=0.006; Fig. 9A), while the combination of miR-99b-5p, miR-409-3p and CEA yielded an AUC of 0.812 (95% CI, 0.679-0.945; sensitivity, 90.9%; specificity, 65.2%; P<0.001; Fig. 9B). The potential miRNA markers evaluated for the diagnosis of early CRC are summarized in Table IX. The diagnostic sensitivity of miR-99b-5p for early CRC achieved a sensitivity consistent with that of CEA. Furthermore, the combination of miR-99b-5p and miR-409-3p yielded a higher diagnostic sensitivity for early CRC compared with that of CEA. However. the combination of miR-99b-5p, miR-409-3p and CEA had 90.9% sensitivity in terms of diagnostic power.

Discussion

With the development of second-generation sequencing technology, it is currently possible to screen for potential biomarkers of various diseases via plasma or serum-derived EV-RNA sequencing, which can then be combined with proteomics technology to comprehensively mine for disease information at both nucleic acid and protein expression levels. One such potential application for this technology is the development of diagnostic markers of early stage of cancer. In the field of biomarker research, liquid biopsy has gained attention due to its rich content, and being readily available and easily sampled, allowing for multiple samplings. However, EVs are particularly favored due to their wide distribution in various types of bodily fluids, abundant contents and ease of stable preservation. Compared with other types of liquid biopsies, EVs can carry biologically active molecules, such as nucleic acids and proteins, which can be used to reflect the information of the parental cells. In addition, such contents are typically protected by the EV phospholipid bilayers and are, therefore, more stable, allowing their preservation for long periods of time (22). Jeppesen *et al* (24) previously reported that exosomes could contain high levels of sRNAs whilst lacking 18S and 28S rRNAs compared with donor cells, and the number of miRNAs was particularly high

Table VII. Abnormally expressed plasma extracellular vesicles-miRNAs in different groups.

Compared group	miRNA	$\log_2$ (fold-change)	P-value
g3 vs. control	hsa-miR-122-5p	-2.61392	0.00275
g4 vs. control	hsa-miR-4433b-3p	1.52970	0.00120
	hsa-miR-122-5p	-2.53459	0.00214
g5 vs. control	hsa-miR-370-3p	1.07430	0.02741
	hsa-miR-654-3p	1.04645	0.01862
	hsa-miR-1180-3p	-1.02473	0.04187
	hsa-miR-451a	-1.28814	0.01713
	hsa-miR-122-5p	-2.41439	0.00037
g5 vs. g4	hsa-miR-543	1.42313	0.00221
	hsa-miR-143-3p	1.08663	0.00347
	hsa-miR-409-3p	1.00511	0.01118
	hsa-miR-127-3p	1.41360	0.00824
	hsa-miR-370-3p	1.26987	0.03325
g5 vs. B79	hsa-miR-625-3p	1.35746	0.02813
	hsa-miR-432-5p	1.32924	0.03362
	hsa-miR-99b-5p	1.19017	0.03783
	hsa-miR-4508	-2.21028	0.01827

g, group no.; miR, microRNA; hsa, *Homo sapiens*.

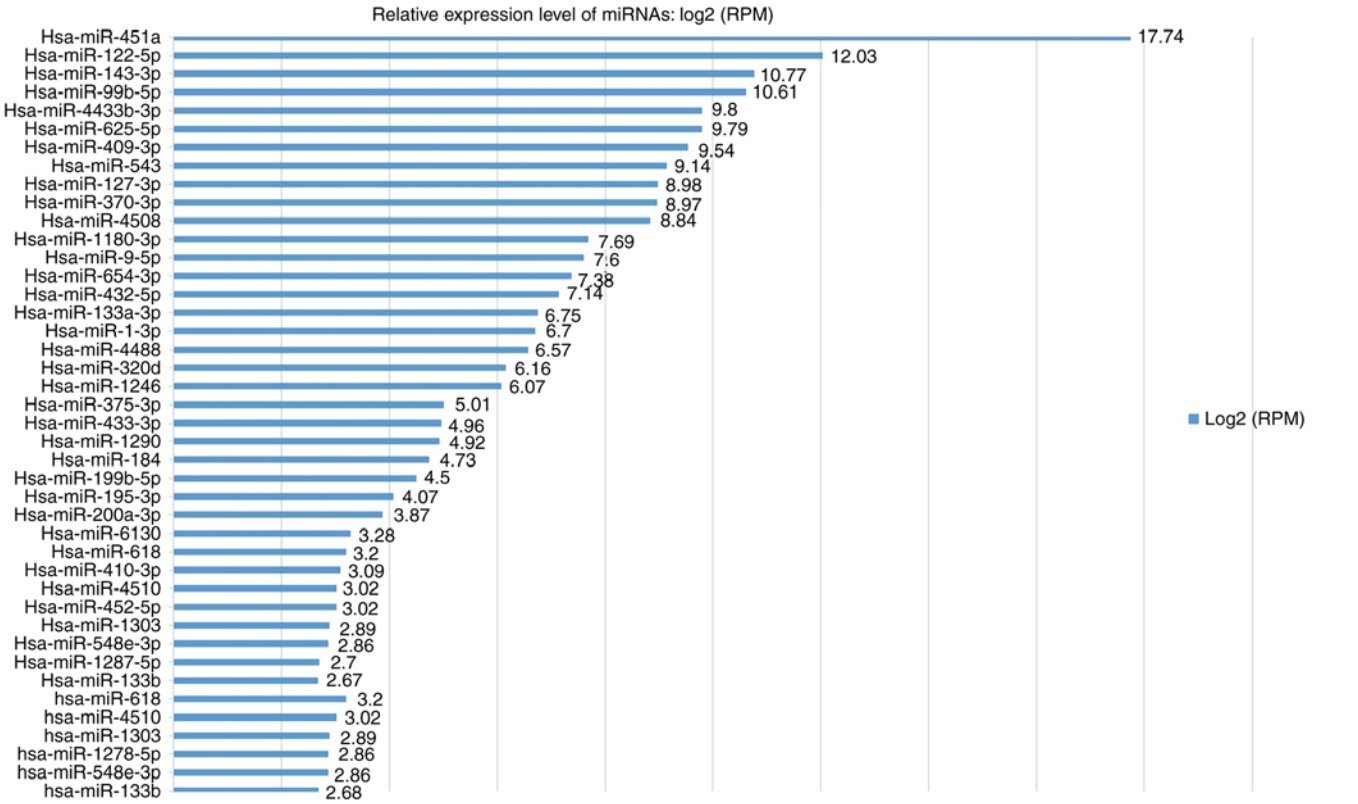

Figure 2. Mean relative expression of miRNAs in 16 plasma extracellular vesicle-RNA samples. miRNA or miR, microRNA; hsa, *Homo sapiens*; RPM, reads per million.

among different types of sRNAs in EVs. Cancer cell-derived EVs have been associated with the tumorigenic potential of epithelial cells (25,26), whilst EV-miRNAs have been found to be capable of promoting tumor development. Previous studies have demonstrated the attractive potential of EVs as diagnostic markers (27,28). Therefore, liquid biopsies are

Table VIII. Association between miRNA expression levels in plasma and clinicopathological characteristics.

	miRNA expression levels (mean ± SD)									
Clinicopathological characteristics	miR-122-5p	P-value	miR-99b-5p	P-value	miR-625-3p	P-value	miR-409-3p	P-value	miR-143-3p	P-value
Gender		0.297		0.861		0.879		0.585		0.132
Male	1.39±1.61		1.39±1.61		1.25±0.87		1.59±1.49		0.82±0.55	
Female	1.95±2.36		1.95±2.36		1.29±1.27		1.87±2.33		1.23±1.12	
Clinical stage		0.354		0.030		0.059		0.997		0.336
0-II	1.90±1.94		1.74±0.98		1.58±1.15		1.70±1.63		0.84±0.52	
III-IV	1.41±1.92		1.23±0.75		1.06±0.88		1.70±1.98		1.07±0.98	
T stage		0.878		0.605		0.902		0.875		0.258
Tis-T2	1.69±2.62		1.57±1.20		1.21±0.84		1.61±1.35		0.72±0.42	
T3-T4	1.59±1.79		1.41±0.81		1.27±1.08		1.72±1.96		1.05±0.90	
N stage		0.606		0.132		0.053		0.871		0.195
N0	1.77±1.81		1.61±0.94		1.51±1.10		1.51±1.10		1.68±1.48	
N1-N2	1.48±2.15		1.24±0.82		1.24±0.82		0.96±0.87		1.60±2.16	
M stage		0.991		0.265		0.443		0.078		0.329
M0	1.60±1.78		1.51±0.92		1.20±0.99		1.35±1.42		0.89±0.62	
M1	1.60±2.30		1.22±0.74		1.44±1.10		2.56±2.44		1.22±1.26	
Lesion site		0.450		0.028		0.446		0.296		0.154
Rectum	1.30±2.14		1.04±0.84		1.11±1.12		1.31±1.31		0.73±0.51	
Colon	1.73±1.83		1.73±1.83		1.34±0.98		1.87±2.01		1.08±0.92	
		0.540		0.085		0.007		0.254		0.383
Right half	1.92±1.23		1.85±0.88		1.80±0.82		2.28±1.92		1.21±0.77	
Light half	1.55±0.93		1.37±0.81		0.97±0.95		1.54±2.03		0.95±1.00	
Differentiation degree		0.861		0.56		0.494		0.909		0.455
High, high-medium	1.59±2.15		1.52±1.05		1.36±1.17		1.65±1.31		0.83±0.45	
Medium, medium-low	1.70±2.00		1.36±0.85		1.15±0.92		1.58±2.09		1.03±1.00	

miRNA/miR, microRNA; SD, standard deviation.

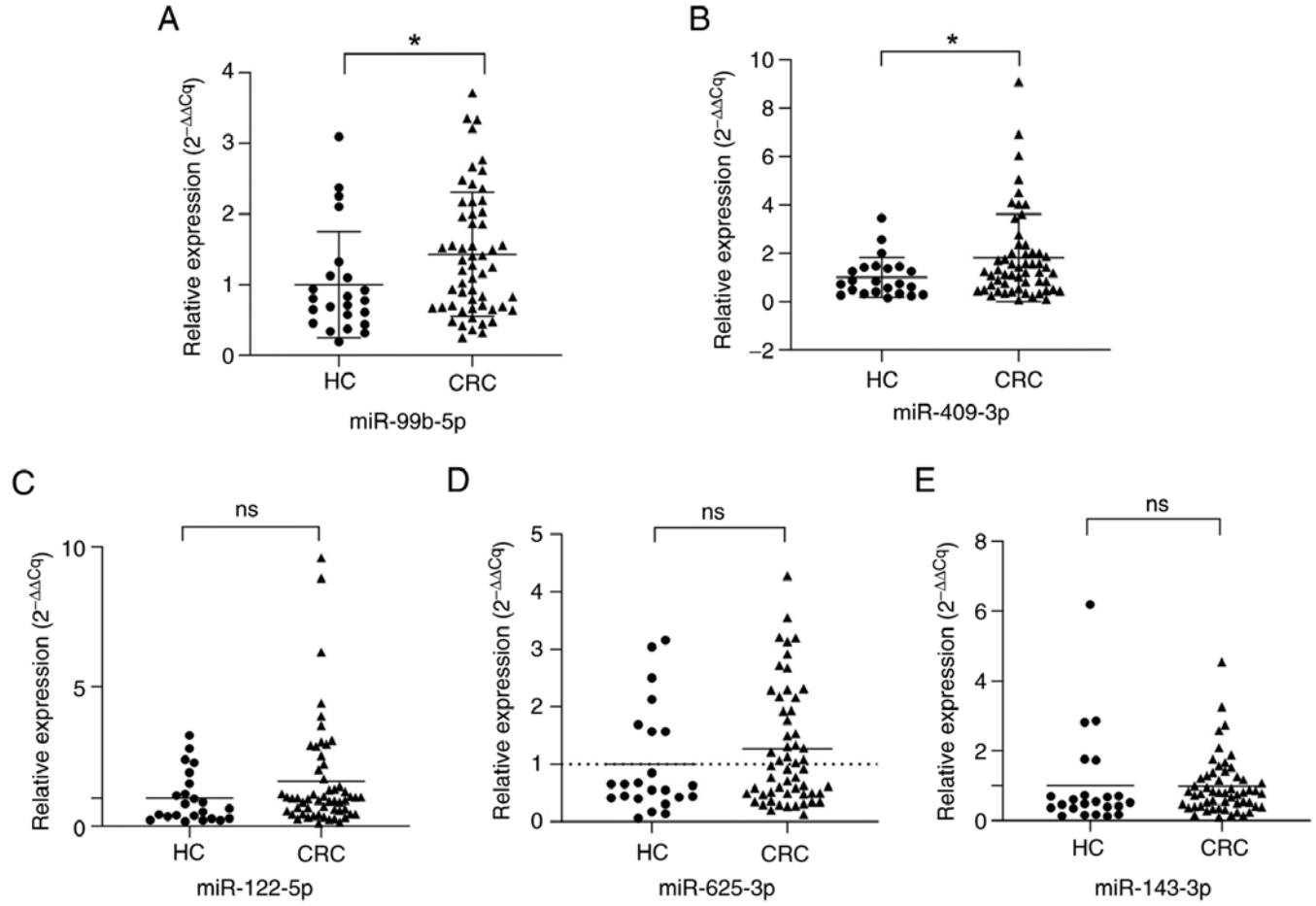

Figure 3. Expression levels of miRNAs in plasma extracellular vesicles. Relative expression of (A) miR-99b-5p, (B) miR-409-3p, (C) miR-122-5p, (D) miR-625-3p and (E) miR-143-3p between different groups. Error bars represent standard deviation. *P<0.05. CRC, colorectal cancer; HC, healthy control; miRNA or miR, microRNA; Cq, quantitative cycle; ns, not significant.

expected to complement currently established methods for the early screening and diagnosis of diseases to facilitate an accurate judgment on patient condition. Future research and technological improvements in the field are expected to increase the clinical value of exosomal miRNAs, since this technology will be cheaper and more convenient compared to existing technologies in the field of exosomes, such as microfluidic techniques and microarray analysis.

In the present study, a panel of differentially expressed miRNAs in CRC plasma EVs was identified and evaluated upon sequencing of ncRNAs isolated from plasma EVs. Considering both expression abundance and FC in expression, five miRNAs, namely miR-122-5p, miR-409-3p, miR-99b-5p, miR-625-3p and miR-143-3p, were validated in plasma EVs from 23 healthy individuals and 56 patients with CRC. A number of miRNAs were found to be expressed at higher levels in the right colon, which may be due to complex differences in the histological structure and vascular microenvironment of CRC at different anatomical locations (26,29). In the present study, it was found that miR-99b-5p and miR-409-3p were highly expressed in CRC compared with healthy individuals. The diagnostic potential of miR-99b-5p for distinguishing early CRC from healthy individuals was assessed using ROC curve analysis, where the AUC was found to be 0.735, with high sensitivity and specificity. It has been previously demonstrated that a signature consisting of multiple combined miRNAs can act as a superior diagnostic marker for disease compared with individual miRNAs (30). The present results support this notion, as demonstrated by the superior power of miR-99b-5p and miR-409-3p in combination, as well as miR-99b-5p, miR-409-3p and CEA in combination, for distinguishing early CRC from healthy individuals. However, additional screening is required in a cohort with suspected CRC to guide clinicians in deciding whether or not to perform further enteroscopy.

To the best of our knowledge, few studies on miR-409-3p have been previously reported, especially in the context of EVs. In CRC, Wang *et al* (31) previously found that miR-409-3p was highly expressed in the plasma samples of patients with CRC compared with the healthy group, which was consistent with the trend observed in EVs in the present study. Previous studies on EV miR-409-3p were mainly performed on other types of cancer, including gastric (32), prostate (33) and ovarian (34) cancer, as well as lung adenocarcinoma (35). Zhou *et al* (35) previously reported that miR-409-3p was highly expressed in plasma EVs isolated from patients with lung adenocarcinoma compared with those from HCs, with a ROC AUC of 0.66. In addition, the AUC of a six-miRNA combination containing miR-409-3p (specifically, miR-19b-3p, miR-21-5p, miR-221-3p, miR-409-3p, miR-425-5p and miR-584-5p) for the diagnosis of lung adenocarcinoma was 0.74 (sensitivity, 67%; specificity, 71%).

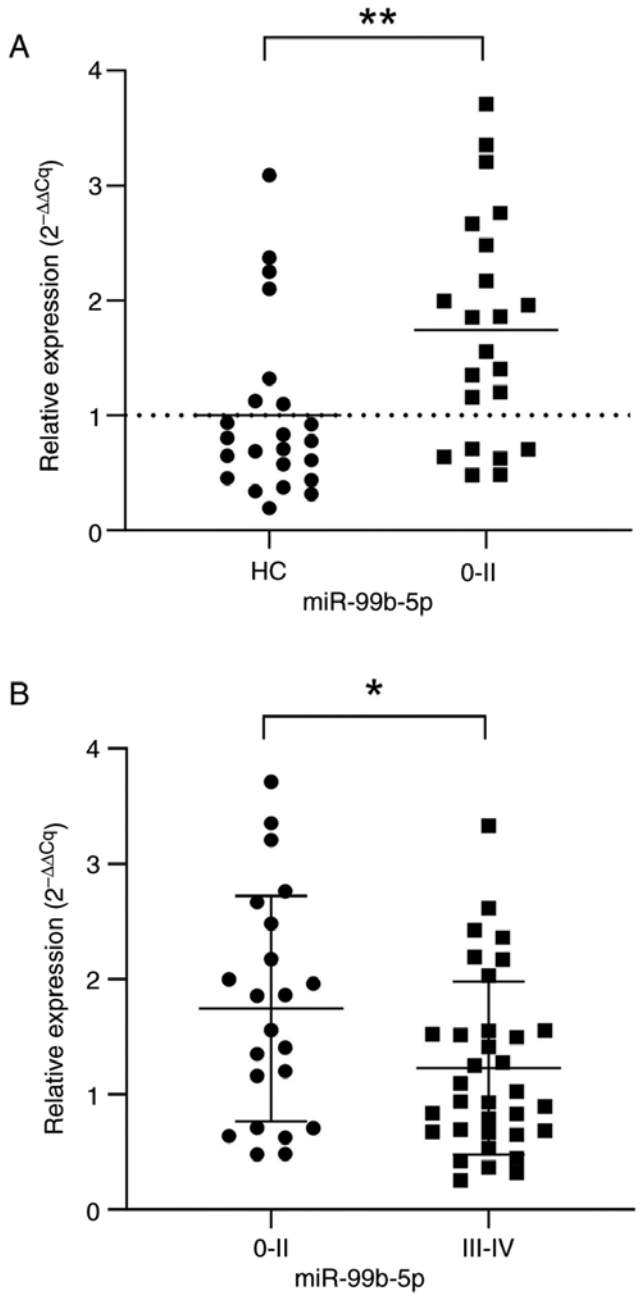

Figure 4. Association of miRNA expression levels with clinicopathological characteristics. (A) Expression levels of miR-99b-5p in colon and rectum. (B) Expression levels of miR-625-3p in left and right colon of patients with colorectal cancer. *P<0.05 and **P<0.01. Data are represented as means ± standard deviation. HC, healthy control; miRNA or miR, microRNA; Cq, quantitative cycle.

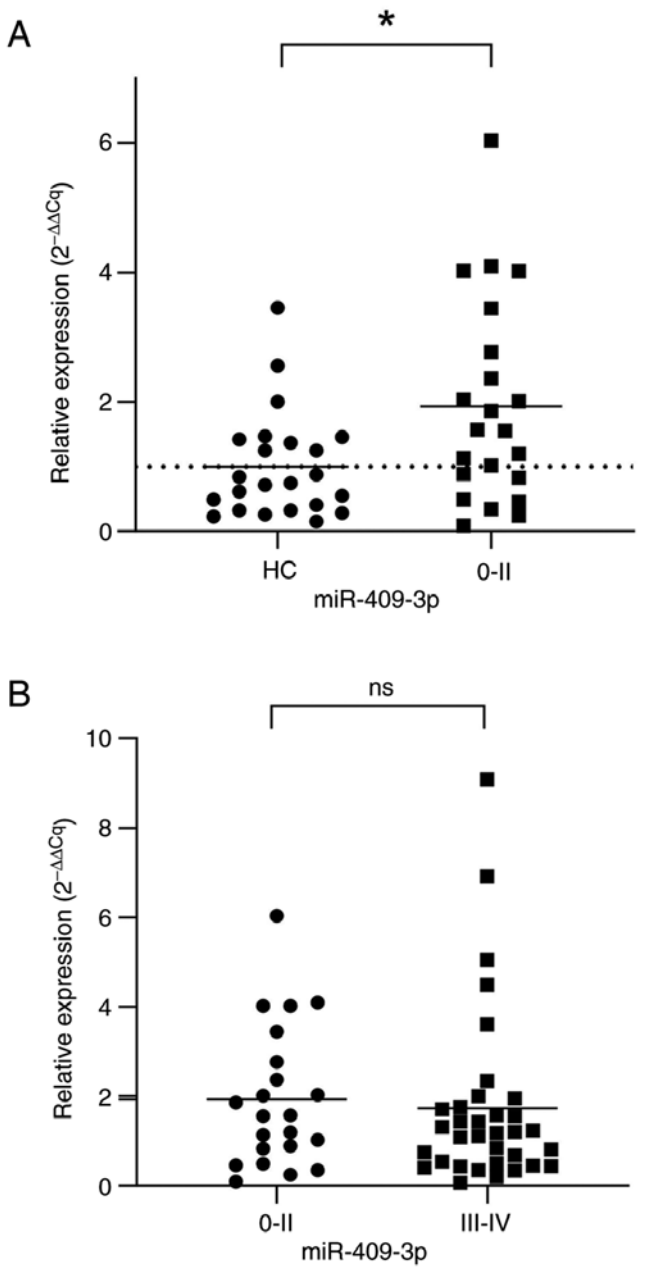

Figure 5. Expression levels of miR-409-3p in plasma EVs. (A) Relative expression of miR-409-3p between the HC group and early CRC group. (B) Relative expression of miR-409-3p between the early CRC group and advanced CRC group. *P<0.05. HC, healthy controls; miRNA or miR, microRNA; Cq, quantitative cycle; ns, not significant.

It has been previously reported that miR-99b-5p expression is dysregulated in a variety of cancer types, including CRC (36), gastric (37), cervical (38), breast (39), oral (40) and ovarian (41) cancer, and non-small-cell lung cancer (NSCLC) (42). However, the association of EV miR-99b-5p with cancer is unclear, although its dysregulation has been reported in CRC (36). miR-99b-5p expression in EVs from patients with ovarian cancer was found to be significantly reduced compared with that in healthy individuals (41). In a sequencing study on 8 patients with NSCLC and 6 healthy individuals, miR-99b-5p expression was found to be downregulated in NSCLC samples compared with healthy individuals (42). In addition, Zhao *et al* (36) reported that, in CRC, miR-99b-5p exhibited low expression levels in serum exosomes, whereas, in the present study, increased miR-99b-5p expression levels were observed in CRC plasma EV.

It is likely that miR-99b-5p may have different expression profiles in different types of tumor, where it may serve a role in either cancer induction or suppression. The reasons underlying the discrepancy between the observations reported by Zhao *et al* (36) and the current findings are unknown. Numerous challenges remain in the development of EV-miRNA markers for the clinical diagnosis of CRC, which may be responsible for differences in the conclusions reported by different studies.

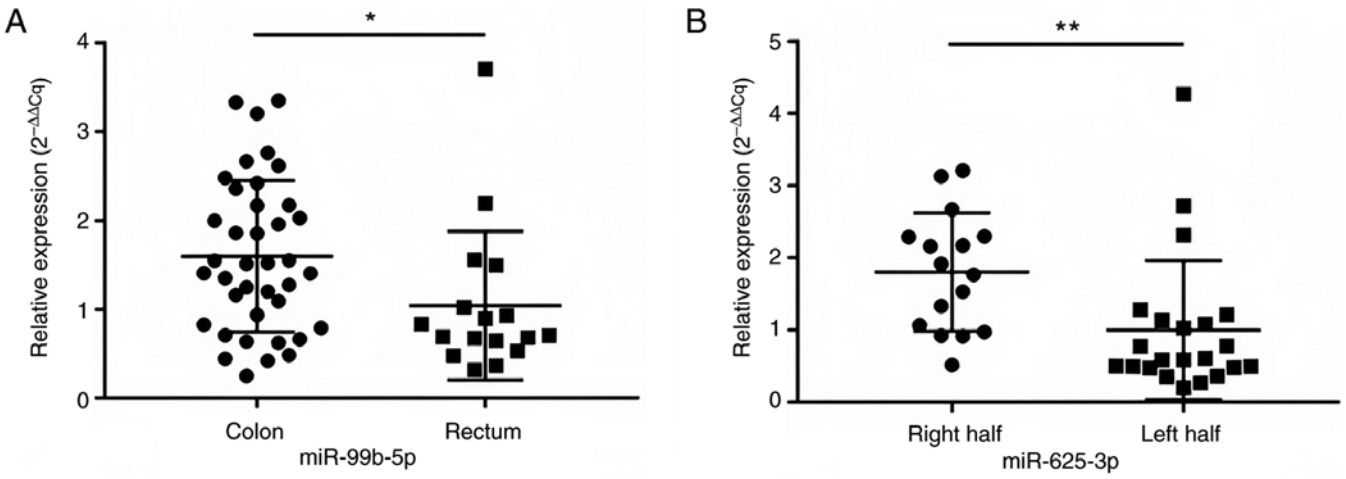

Figure 6. Analysis of miRNA expression levels and clinicopathologic characteristics of CRC. (A) Expression levels of miR-99b-5p in the colon and rectum. (B) Expression levels of miR-625-3p in the left and right colon of CRC. *P<0.05 and **P<0.01. HC, healthy controls; miRNA or miR, microRNA; Cq, quantitative cycle.

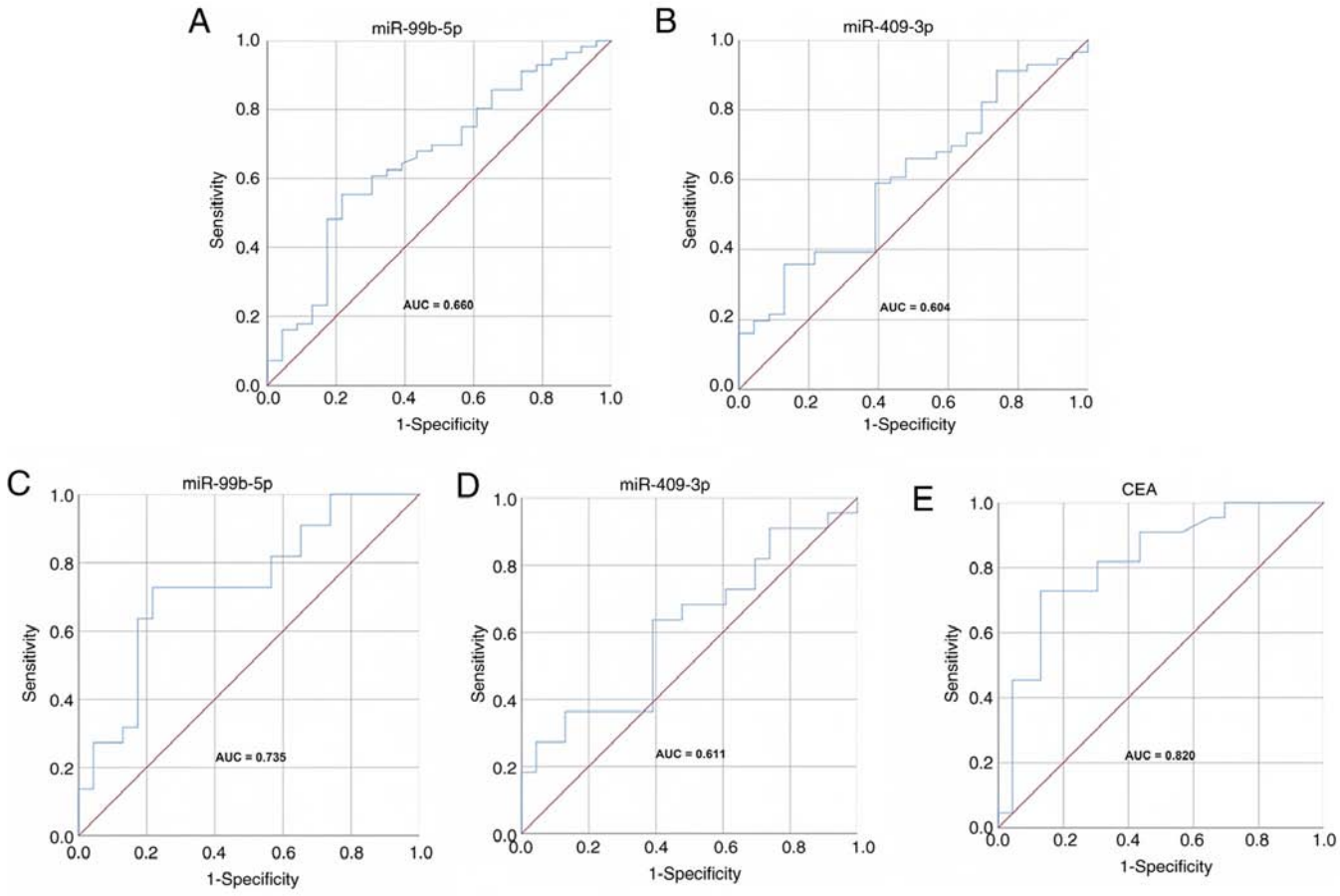

Figure 7. ROC curve analysis of the diagnostic potential of individual miRNAs for CRC. ROC curve analysis of (A) miR-99b-5p and (B) miR-409-3p for diagnosis of CRC. ROC curve analysis of (C) miR-99b-5p and (D) miR-409-3p for diagnosis of early CRC. (E) ROC curve analysis of CEA for diagnosis of early CRC and healthy controls. ROC, receiver operating characteristic; miRNA or miR, microRNA; CRC, colorectal cancer; CEA, carcinoembryonic antigen.

The present study has a number of limitations, including differences in collection, processing and storage of study samples, differential analysis methods, systems and instruments compared with previous studies, which can impact the results. EVs were introduced into the 'Minimal information for studies of extracellular vesicles 2018 (MISEV2018)' guidelines in 2018 (43), which aimed to establish a minimum standard in the field of EV research. This guideline was used as a reference in the present study. In addition, inter-individual variability of clinical samples could have been mitigated with larger sample sizes collected from multiple centers. However, clinical samples are limited and not easily accessible. The impact of other systemic diseases must also be considered, as Pinel *et al* (44) showed that miRNA passenger

Table IX. Diagnostic potential of miRNAs, CEA and miRNA combinations for colorectal cancer.

miRNA/tumor marker	AUC	95% CI (range)	Sensitivity, %	Specificity, %	P-value
miR-99b-5p	0.735	0.587-0.884	72.7	78.3	0.007
miR-409-3p	0.611	0.443-0.778	63.6	60.9	0.204
CEA	0.820	0.695-0.945	72.7	87.0	<0.001
miR-99b-5p and miR-409-3p	0.741	0.592-0.891	77.3	78.3	0.006
miR-99b-5p, miR-409-3p and CEA	0.812	0.679-0.945	90.9	65.2	<0.001

miRNA/miR, microRNA; AUC, area under the curve; CI, confidence interval; CEA, carcinoembryonic antigen.

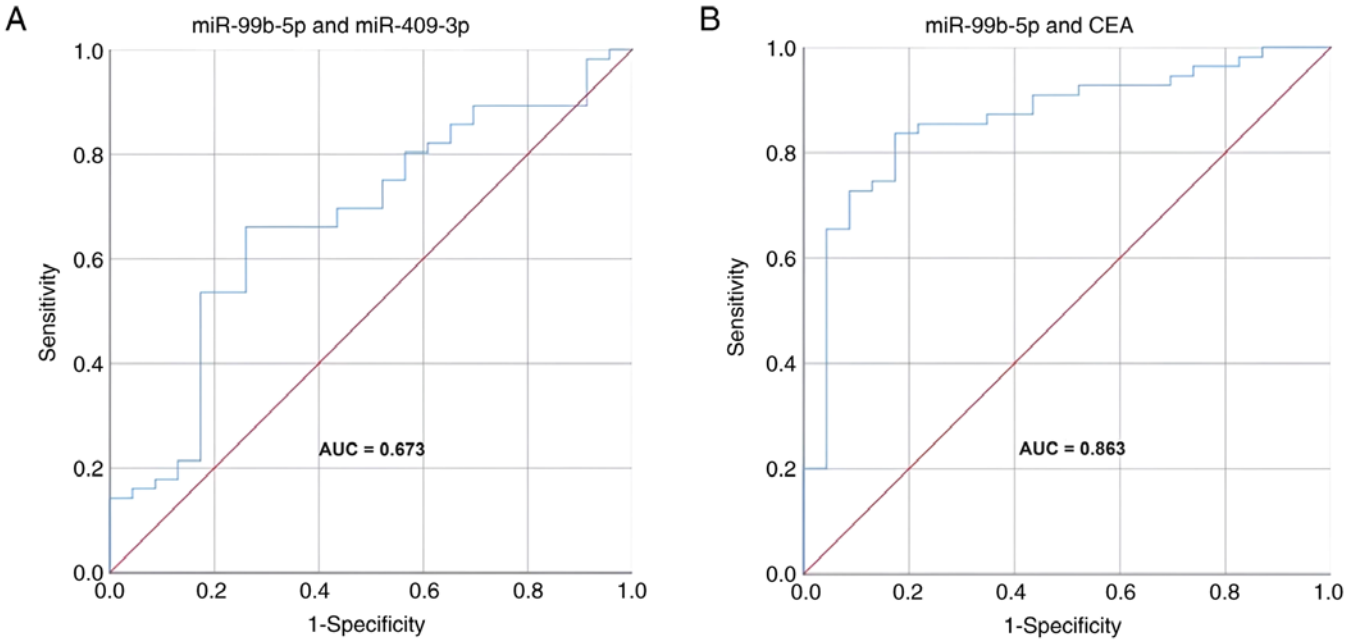

Figure 8. Receiver operating characteristic curves were employed to analyze the differential diagnostic potential of miRNA combinations for colorectal cancer and healthy controls. (A) miR-99b-5p and miR-409-3p combination. (B) miR-99b-5p and CEA combination. miR, microRNA; CEA, carcinoembryonic antigen.

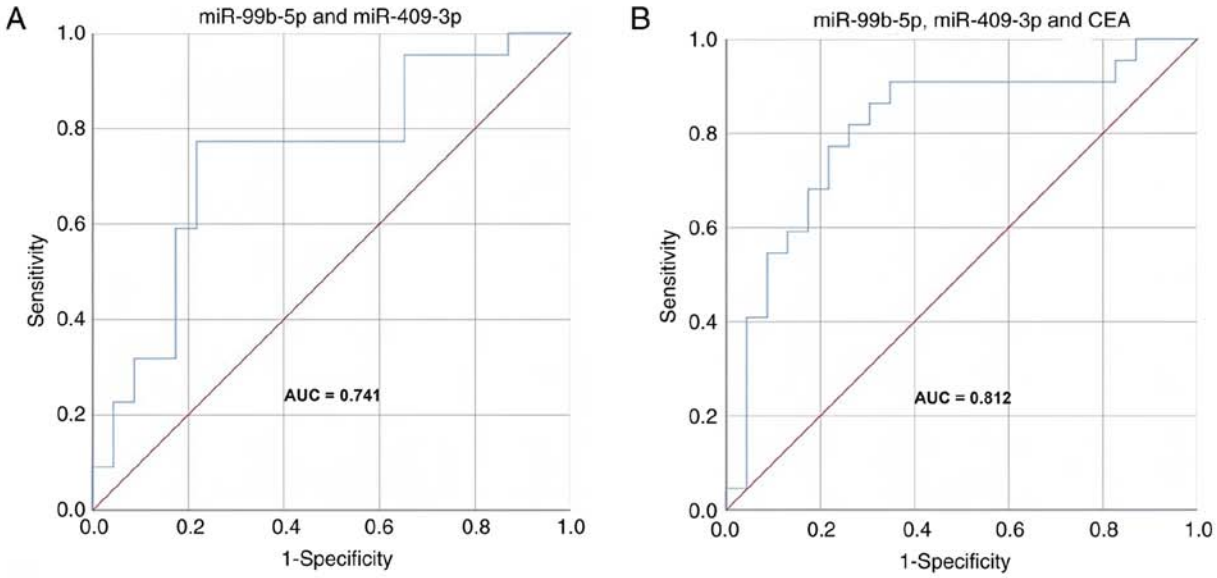

Figure 9. Receiver operating characteristic curve analysis of the differential diagnostic potential of miRNA combinations for early colorectal cancer and healthy controls. (A) miR-99b-5p and miR-409-3p combination. (B) miR-99b-5p, miR-409-3p and CEA combination. miR, microRNA; CEA, carcinoembryonic antigen.

strands were frequently dysregulated in acute vascular injury, which suggests that the impact of cardiovascular disease on the expression of miRNAs is an important consideration. At present, the exact physiological function of EVs in cancer remains unclear, warranting further investigation. Therefore, various aspects of EV physiology, including the occurrence, specific functions and mechanism of action of EVs, as well as the selection, transport and mechanism of action of EV contents, remain to be fully elucidated. In addition, although miRNA combinations were found to exert a potential role in predicting CRC in the current study, additional cases and studies are required to confirm its specificity.

In conclusion, the present study found that miR-409-3p and miR-99b-5p were highly expressed in CRC plasma EVs, where the combination of miR-99b-5p and miR-409-3p, in addition to the combination of miR-99b-5p, miR-409-3p and CEA, provided high diagnostic sensitivity for early CRC. However, the present study was based on a limited sample size. Although the current study found that these miRNAs had a potential role in predicting disease, due to individual variability in humans, a multi-center study with increased sample size is required to further verify their diagnostic sensitivity and specificity. Conducting in-depth molecular mechanistic studies would certainly improve the current understanding on the functional roles of miR-409-3p and miR-99b-5p in CRC.

Acknowledgements

Not applicable.

Funding

The present study was funded by the Fund for Scientific and Technological Innovation and Development in Guangzhou (grant no. 201904010394), and School of Aerospace Medicine, Air Force Military Medical University (grant no. 2024HYYH07).

Availability of data and materials

The data generated in the present study may be requested from the corresponding author.

Authors' contributions

LZ and CZ confirm the authenticity of all the raw data. XX, LZ and CZ participated in the conception and design of the study. LZ performed all the experiments with help from CZ. LZ, CZ, QH and SJ performed statistical analyses. TP, SW and XX reviewed and validated the statistical analysis results. CZ wrote and revised the manuscript. All authors read and approved the final version of the manuscript.

Ethics approval and consent to participate

The present prospective study was approved by The Ethics Committee of the Third Affiliated Hospital of Guangzhou Medical University, including the use of all datasets (approval no. 2017.117). Written informed consent was obtained from all participants.

Patient consent for publication

Not applicable.

Competing interests

The authors declare that they have no competing interests.

References

1. Sung H, Ferlay J, Siegel RL, Laversanne M, Soerjomataram I, Jemal A and Bray F: Global cancer statistics 2020: GLOBOCAN estimates of incidence and mortality worldwide for 36 cancers in 185 countries. CA Cancer J Clin 71: 209-249, 2021.
2. Chen W, Zheng R, Baade PD, Zhang S, Zeng H, Bray F, Jemal A, Yu XQ and He J: Cancer statistics in China, 2015. CA Cancer J Clin 66: 115-132, 2016.
3. Kemeny N: The management of resectable and unresectable liver metastases from colorectal cancer. Curr Opin Oncol 22: 364-373, 2010.
4. Norén A, Eriksson HG and Olsson LI: Selection for surgery and survival of synchronous colorectal liver metastases; a nationwide study. Eur J Cancer 53: 105-114, 2016.
5. Zhang J, Cheng Z, Ma Y, He C, Lu Y, Zhao Y, Chang X, Zhang Y, Bai Y and Cheng N: Effectiveness of screening modalities in colorectal cancer: A network Meta-Analysis. Clin Colorectal Cancer 16: 252-263, 2017.
6. Rex DK, Boland CR, Dominitz JA, Giardiello FM, Johnson DA, Kaltenbach T, Levin TR, Lieberman D and Robertson DJ: Colorectal cancer screening: Recommendations for physicians and patients from the U.S. Multi-Society task force on colorectal cancer. Gastroenterology 153: 307-323, 2017.
7. Benson AB, Venook AP, Al-Hawary MM, Cederquist L, Chen YJ, Ciombor KK, Cohen S, Cooper HS, Deming D, Engstrom PF, *et al*: Rectal cancer, Version 2 .2018, NCCN clinical practice guidelines in oncology. J Natl Compr Canc Netw 16: 874-901, 2018.
8. Breitenbuecher F, Hoffarth S, Worm K, Cortes-Incio D, Gauler TC, Köhler J, Herold T, Schmid KW, Freitag L, Kasper S and Schuler M: Development of a highly sensitive and specific method for detection of circulating tumor cells harboring somatic mutations in non-small-cell lung cancer patients. PLoS One 9: e85350, 2014.
9. Hill M and Tran N: miRNA interplay: Mechanisms and consequences in cancer. Dis Model Mech 14: dmm047662, 2021.
10. Molnár B, Galamb O, Kalmár A, Barták BK, Nagy ZB, Tóth K, Tulassay Z, Igaz P and Dank M: Circulating cell-free nucleic acids as biomarkers in colorectal cancer screening and diagnosis-an update. Expert Rev Mol Diagn 19: 477-498, 2019.
11. Slattery ML, Herrick JS, Mullany LE, Wolff E, Hoffman MD, Pellatt DF, Stevens JR and Wolff RK: Colorectal tumor molecular phenotype and miRNA: expression profiles and prognosis. Mod Pathol 29: 915-927, 2016.
12. Milane L, Singh A, Mattheolabakis G, Suresh M and Amiji MM: Exosome mediated communication within the tumor microenvironment. J Control Release 219: 278-294, 2015.
13. Grigoryeva ES, Savelieva OE, Popova NO, Cherdyntseva NV and Perelmuter VM: Do tumor exosome integrins alone determine organotropic metastasis? Mol Biol Rep 47: 8145-8157, 2020.
14. Chen M, Xu R, Rai A, Suwakulsiri W, Izumikawa K, Ishikawa H, Greening DW, Takahashi N and Simpson RJ: Distinct shed microvesicle and exosome microRNA signatures reveal diagnostic markers for colorectal cancer. PLos One 14: e0210003, 2019.
15. Amin MB, Edge SB, Greene FL, Byrd DR, Brookland RK, Washington MK, Gershenwald JE, Compton CC, Hess KR, Sullivan DC, *et al*: AJCC cancer staging manual 8th Edition. Springer, New York, NY, 252-274, 2017.
16. Kozomara A and Griffiths-Jones S: miRBase: Annotating high confidence microRNAs using deep sequencing data. Nucleic Acids Res 42: D68-D73, 2014.
17. Kalvari I, Nawrocki EP, Ontiveros-Palacios N, Argasinska J, Lamkiewicz K, Marz M, Griffiths-Jones S, Toffano-Nioche C, Gautheret D, Weinberg Z, *et al*: Rfam 14: Expanded coverage of metagenomic, viral and microRNA families. Nucleic Acids Res 49: D192-D200, 2021.

18. Sai Lakshmi S and Agrawal S: piRNABank: A web resource on classified and clustered Piwi-interacting RNAs. Nucleic Acids Res 36: D173-D177, 2008.
19. Robinson MD, McCarthy DJ and Smyth GK: edgeR: A Bioconductor package for differential expression analysis of digital gene expression data. Bioinformatics 26: 139-140, 2010.
20. Livak KJ and Schmittgen TD: Analysis of relative gene expression data using real-time quantitative PCR and the 2(-Delta Delta C(T)) method. Methods 25: 402-408, 2001.
21. Davoren PA, McNeill RE, Lowery AJ, Kerin MJ and Miller N: Identification of suitable endogenous control genes for microRNA gene expression analysis in human breast cancer. BMC Mol Biol 9: 76, 2008.
22. Raposo G and Stoorvogel W: Extracellular vesicles: Exosomes, microvesicles, and friends. J Cell Biol 200: 373-383, 2013.
23. Baran B, Mert Ozupek N, Yerli Tetik N, Acar E, Bekcioglu O and Baskin Y: Difference between left-sided and right-sided colorectal cancer: A focused review of literature. Gastroenterology Res 11: 264-273, 2018.
24. Jeppesen DK, Fenix AM, Franklin JL, Higginbotham JN, Zhang Q, Zimmerman LJ, Liebler DC, Ping J, Liu Q, Evans R, *et al*: Reassessment of exosome composition. Cell 177: 428-445.e18, 2019.
25. Antonyak MA, Li B, Boroughs LK, Johnson JL, Druso JE, Bryant KL, Holowka DA and Cerione RA: Cancer cell-derived microvesicles induce transformation by transferring tissue transglutaminase and fibronectin to recipient cells. Proc Natl Acad Sci USA 108: 4852-4857, 2011.
26. Melo SA, Sugimoto H, O'Connell JT, Kato N, Villanueva A, Vidal A, Qiu L, Vitkin E, Perelman LT, Melo CA, *et al*: Cancer exosomes perform cell-independent microRNA biogenesis and promote tumorigenesis. Cancer Cell 26: 707-721, 2014.
27. van Niel G, D'Angelo G and Raposo G: Raposo, Shedding light on the cell biology of extracellular vesicles. Nat Rev Mol Cell Biol 19: 213-228, 2018.
28. Shen M, Di K, He H, Xia Y, Xie H, Huang R, Liu C, Yang M, Zheng S, He N and Li Z: Progress in exosome associated tumor markers and their detection methods. Mol Biomed 1: 3, 2020.
29. Hanahan D and Coussens LM: Accessories to the crime: Functions of cells recruited to the tumor microenvironment. Cancer Cell 21: 309-322, 2012.
30. Yuan T, Huang X, Woodcock M, Du M, Dittmar R, Wang Y, Tsai S, Kohli M, Boardman L, Patel T and Wang L: Plasma extracellular RNA profiles in healthy and cancer patients. Sci Rep 6: 19413, 2016.
31. Wang S, Xiang J, Li Z, Lu S, Hu J, Gao X, Yu L, Wang L, Wang J, Wu Y, *et al*: A plasma microRNA panel for early detection of colorectal cancer. Int J Cancer 136: 152-161, 2015.
32. Yu L, Xie J, Liu X, Yu Y and Wang S: Plasma exosomal CircNEK9 accelerates the progression of gastric cancer via miR-409-3p/MAP7 axis. Dig Dis Sci 66: 4274-4289, 2021.
33. Yu Q, Li P, Weng M, Wu S, Zhang Y, Chen X, Zhang Q, Shen G, Ding X and Fu S: Nano-Vesicles are a potential tool to monitor therapeutic efficacy of carbon ion radiotherapy in prostate cancer. J Biomed Nanotechnol 14: 168-178, 2018.
34. Zhang S, Zhang X, Fu X, Li W, Xing S and Yang Y: Identification of common differentially-expressed miRNAs in ovarian cancer cells and their exosomes compared with normal ovarian surface epithelial cell cells. Oncol Lett 16: 2391-2401, 2018.
35. Zhou X, Wen W, Shan X, Zhu W, Xu J, Guo R, Cheng W, Wang F, Qi LW, Chen Y, *et al*: A six-microRNA panel in plasma was identified as a potential biomarker for lung adenocarcinoma diagnosis. Oncotarget 8: 6513-6525, 2017.
36. Zhao YJ, Song X, Niu L, Tang Y, Song X and Xie L: Circulating exosomal miR-150-5p and miR-99b-5p as diagnostic biomarkers for colorectal cancer. Front Oncol 9: 1129, 2019.
37. Wang Z, Zhao Z, Yang Y, Luo M, Zhang M, Wang X, Liu L, Hou N, Guo Q, Song T, *et al*: MiR-99b-5p and miR-203a-3p function as tumor suppressors by targeting IGF-1R in gastric cancer. Sci Rep 8: 10119, 2018.
38. Li YJ, Wang Y and Wang YY: MicroRNA-99b suppresses human cervical cancer cell activity by inhibiting the PI3K/AKT/mTOR signaling pathway. J Cell Physiol 234: 9577-9591, 2019.
39. Worst TS, Previti C, Nitschke K, Diessl N, Gross JC, Hoffmann L, Frey L, Thomas V, Kahlert C, Bieback K, *et al*: miR-10a-5p and miR-29b-3p as extracellular vesicle-associated prostate cancer detection markers. Cancers (Basel) 12: 43, 2019.
40. He K, Tong D, Zhang S, Cai D, Wang L, Yang Y, Gao L, Chang S, Guo B, Song T, *et al*: miRNA-99b-3p functions as a potential tumor suppressor by targeting glycogen synthase kinase-3β in oral squamous cell carcinoma Tca-8113 cells. Int J Oncol 47: 1528-1536, 2015.
41. Zhang H, Xu S and Liu X: MicroRNA profiling of plasma exosomes from patients with ovarian cancer using high-throughput sequencing. Oncol Lett 17: 5601-5607, 2019.
42. Wang L, Wang L and Zhu J: Serum exosomal microRNAs as predictive markers for EGFR mutations in non-small-cell lung cancer. J Clin Lab Anal 35: e23743, 2021.
43. Thery C, Witwer KW, Aikawa E, Alcaraz MJ, Anderson JD, Andriantsitohaina R, Antoniou A, Arab T, Archer F, Atkin-Smith G, *et al*: Minimal information for studies of extracellular vesicles 2018 (MISEV2018): A position statement of the International Society for Extracellular Vesicles and update of the MISEV2014 guidelines. J Extracell Vesicles 7: 1535750, 2018.
44. Pinel K, Diver LA, White K, McDonald RA and Baker AH: Substantial Dysregulation of miRNA passenger strands underlies the vascular response to injury. Cell 8: 83, 2019.